SLAC – PUB – 3730
July 1985
(T/E)

RADIATIVE J/ψ DECAYS AND THE PSEUDOSCALAR PUZZLE*

NORBERT WERMES†

Stanford Linear Accelerator Center
Stanford University, Stanford, California, 94305

ABSTRACT

Recent results on radiative decays of the J/ψ, obtained by the SPEAR detectors Mark III and Crystal Ball and the DCI detector DM2 at Orsay, are presented. The status of the glueball candidates $\theta(1690)$, $\iota(1460)$, and $\xi(2200)$, and the decays $J/\psi \to \gamma$ Vector Vector are reviewed. A coupled channel analysis of $\iota(1460)$ decays to $K\bar{K}\pi$, $\rho\rho$, $\omega\omega$, and $\gamma\rho$ is presented which may help to understand the pseudoscalar sector in radiative J/ψ decays.

Invited Talk presented at the Physics in Collision V Conference,
Autun, France, July 3-5, 1985

* Work supported in part by the Department of Energy, contract number DE–AC03–76SF00515, and by the Alexander von Humboldt Foundation.
† Present address: E.P. Division, CERN, 1211 Geneva 23, Switzerland.

1. Introduction

The J/ψ is expected to be an ideal place to search for glueballs. It is a pure flavour singlet state and its radiative decays are supposed to proceed mainly through annihilation into the radiative photon and two gluons. QCD inspired models such as the bag model, lattice gauge theories, and string potential models predict the lowest lying glueballs to have masses well below 3 GeV.[1]

The main decay mechanisms of the J/ψ are depicted in Fig. 1. The radiative process (Fig. 1(c)) occurs in about 8% of all J/ψ decays. Although the mass spectrum for glueballs can be calculated in various models[1] precise predictions of glueball characteristics, which could help the experimenters to find such states, do not exist. Complications arise from the fact that glueballs are likely to mix with nearby $q\bar{q}$ or with $q\bar{q}g$ or $q\bar{q}q\bar{q}$ states which are expected to exist in the same mass region. A list of features expected for glueballs provides some qualitative guidance for the search for candidate states.

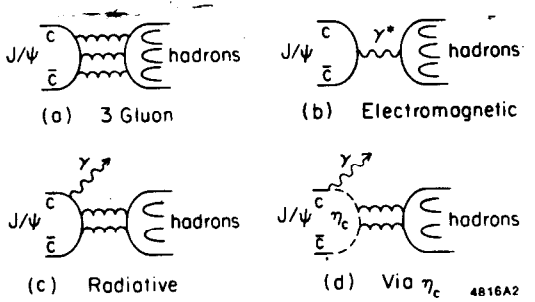

Fig. 1. Lowest order diagrams for ψ decay. a) hadronic decay, b) electromagnetic decay, c) radiative decay to gluons d) radiative transition to the η_c.

- If accessible through radiative J/ψ decays, glueballs are expected to be copiously produced compared to the production of pure $q\bar{q}$ states. The η, which appears to have no strong glue component,[2] is produced in radiative J/ψ decays with a branching fraction of about 0.1%.
- Since bound states of gluons do not carry quark flavour their decays should occur in a flavour symmetric way. While this is true for the glueball–quark couplings the actual decay rates will depend on the available phase space and possible helicity suppression effects.
- Additional help for identifying glueball candidates of a given spin-parity can be obtained from the existing SU(3) $q\bar{q}$ nonets for groundstate and excitated states. If there is no

room left in the $q\bar{q}$ multiplets the glueball hypothesis becomes more likely. A resonance with exotic J^{PC} quantum numbers (e.g. 1^{-+}) would rule out any $q\bar{q}$ assignment.

- Copious production of a candidate state in hadronic J/ψ decay such as $J/\psi \to (\omega, \phi, \eta) + X$, which occurs through diagrams as Fig. 1(a), and a small branching fraction in radiative J/ψ decay implies that the state probably has a $q\bar{q}$ component and is therefore not pure gluonium.
- According to the glueball lore the width of glueballs should follow the $\sqrt{OZI}$ rule.[5] This rule is derived from the observation that in OZI forbidden meson decays the quarks annihilate into three gluons which then mediate the decay. In contrast, a glueball decay does not have to proceed through quark annihilation. This naive argument has been criticized on several grounds[4] and, lacking any detailed calculation, one can only state that the width of glueballs is not known to any precision and could be anywhere between a few MeV and a few hundred MeV.
- A perturbative QCD calculation by Billoire et al.[6] using massless gluons predicts dominance of spin-parities 2^{++}, 0^{++}, and 0^{-+} for the gg system in $J/\psi \to \gamma gg$.

Figure 2 shows the inclusive photon energy spectrum as measured by the Crystal Ball detector.[6] The spectrum is very rich with resonances showing the presence of η, η', $f(1270)$, and $\iota(1460)$. Since η, η', and $f(1270)$ are known to be members of the pseudoscalar and tensor $q\bar{q}$ multiplets one sees that not every resonance produced in radiative J/ψ decays is a glueball candidate.

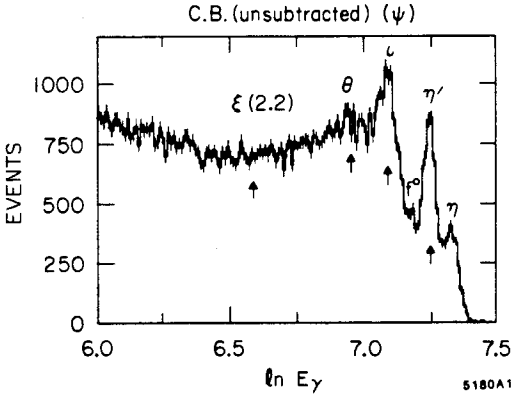

Fig. 2. Energy distribution of photons from $J/\psi \to \gamma + X$ (Crystal Ball).

The strongest candidates for glueballs produced in radiative J/ψ decays are $\theta(1690)$, $\iota(1460)$, and $\xi(2200)$. The parameters of these candidates are given in Table I. The three tensor states $g_T(2120)$, $g_T(2220)$, and $g_T(2360)$,[7] observed in $\pi^- p \to \phi\phi n$ reactions have been interpreted as glueballs, but they have as yet not been observed in $J/\psi \to \gamma$X.

TABLE I

	Parameter	Mark II	Crystal Ball	Mark III	DM2
	Number of prod. J/ψ ($\times 10^6$)	1.3	2.2	2.7 + (3.2)	8.6
$\theta(1690)$	mass (MeV)	1700 ± 30	1670 ± 50	1720 ± 10	1707 ± 10
	Γ (MeV)	156 ± 20	160 ± 80	130 ± 20	166 ± 33
	J^{PC}		2^{++}	2^{++}	$0^{++}/2^{++}$
	$B_\psi \cdot B(\theta \to \eta\eta) \times 10^4$		3.8 ± 1.6		
	$B_\psi \cdot B(\theta \to K^+K^-) \times 10^4$	$6.0 \pm 0.9 \pm 2.5$		$4.8 \pm 0.6 \pm 0.9$	$4.6 \pm 0.7 \pm 0.7$
	$B_\psi \cdot B(\theta \to \pi^+\pi^-) \times 10^4$			$1.6 \pm 0.4 \pm 0.3$	2.0 ± 0.7
	$B(\psi \to \gamma\theta)$			$> 1.6 \times 10^3$	
$\iota(1460)$	mass (MeV)	$1440 \pm^{10}_{15}$	$1440 \pm^{20}_{15}$	$1456 \pm 5 \pm 6$	$1460 \pm 3 \pm 8$
	Γ (MeV)	$50 \pm^{30}_{20}$	$55 \pm^{20}_{30}$	$95 \pm 10 \pm 15$	$100 \pm 12 \pm 15$
	J^{PC}		0^{-+}	0^{-+}	0^{-+} consistent
	$B_\psi \cdot B(\iota \to K\bar{K}\pi) \times 10^3$	4.3 ± 1.7	$4.0 \pm 0.7 \pm 1.0$	$5.0 \pm 0.3 \pm 0.8$	$3.9 \pm 0.06 \pm 0.9$
	mass in $\gamma\rho$ (MeV)		1390 ± 25	$1420 \pm 15 \pm 20$	1401 ± 18
	Γ (MeV)		$185 \pm^{110}_{80}$	$133 \pm 55 \pm 30$	174 ± 44
	$B_\psi \cdot B(\iota \to \gamma\rho^\circ) \times 10^4$		$1.9 \pm 0.5 \pm 0.4$	$1.0 \pm 0.2 \pm 0.2$	$0.9 \pm 0.2 \pm 0.14$
$\xi(2218)$	mass (MeV)			$2218 \pm 3 \pm 10$	
	Γ (MeV)			< 40 (95% *C.L.*)	
	$B_\psi \cdot B(\xi \to K^+K^-) \times 10^5$			$3.8 \pm 1.3 \pm 0.9$	< 1.2 (95% *C.L.*)

Some of the experiments which have taken data on the J/ψ resonance are listed in Table I. Only DM2 at the DCI storage ring in ORSAY and Mark III at SPEAR are analyzing recent data. Therefore I will mostly present data and analyses from these two experiments. The status of the candidate states seen in J/ψ radiative decays are discussed in section 2 and 3. Measurements of $J/\psi \to \gamma$ Vector Vector are reported in section 4. The pseudoscalar puzzle is introduced in section 5 and a coupled channed analysis of $\iota(1460)$ decays is presented in section 6. The conclusions are summarized in section 7.

2. $\xi(2200)$ and $\theta(1690)$

I will only very briefly comment on the status of the elusive $\xi(2200)$ particle. A narrow peak in the $K\bar{K}$ mass distribution of $J/\psi \to \gamma K^+K^-$ was found by Mark III[8,9] at 2.218 GeV with a branching fraction of $B(J/\psi \to \gamma\xi)B(\xi \to K^+K^-) = (3.8 \pm 1.3 \pm 0.9) \times 10^{-5}$. This observation was based on a sample of 2.7×10^6 produced J/ψ. The DM2 collaboration does not observe such a signal quoting a 95% confidence level upper limit of $B(J/\psi \to \gamma\xi)B(\xi \to K^+K^-) < 1.2 \times 10^{-5}$. The K^+K^- invariant mass distributions for both experiments are shown in Fig. 3. The Mark III experiment has doubled its statistics in a recent data run. The data are presently being processed. New results are not yet available.

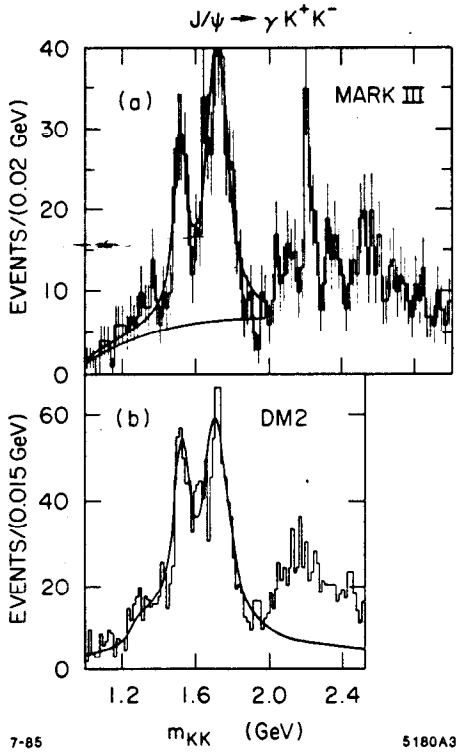

Fig. 3. Invariant $K\bar{K}$ mass distributions from Mark III (a) and DM2 (b).

The $\theta(1690)$[10] is seen by both DM2 and Mark III (Fig. 3), clearly separated from the $f'(1515)$. The decay $\theta(1690) \to \pi^+\pi^-$ is evident from the Mark III data shown in Fig. 4. The total branching fraction for $J/\psi \to \gamma\theta(1690)$, obtained by summing the $\eta\eta$, $K\bar{K}$, and $\pi\pi$ decay modes and assuming the θ to be an isosinglet, is at least 1.6×10^{-3}.

An important result, which might be interesting with respect to the evaluation of the glueball nature of the $\theta(1690)$, are the polarisation measurements of $f(1270)$, $f'(1515)$, and $\theta(1690)$. The direct comparison of the $q\bar{q}$ tensor mesons f and f' with the $\theta(1690)$, which also

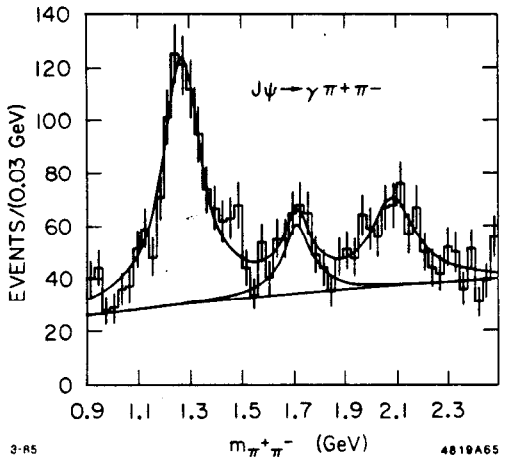

Fig. 4. Invariant $\pi\pi$ mass distribution (Mark III) showing evidence for the decay $J/\psi \to \gamma\theta$, $\theta \to \pi\pi$.

has $J^{PC} = 2^{++}$, shows that the $\theta(1690)$ is produced with equal strengths in helicities 0, 1, and 2 and a 180° phase difference, $(A_1/A_0, A_2/A_0) = (-1, -1)$. In contrast, the f and f' are produced very differently with $(A_1/A_0, A_2/A_0) = (1, 0)$, i.e. there is no helicity 2 contribution. This result is shown in Fig. 5. Table II shows the experimental measurements in comparison with theoretical calculations. The DM2 results in Table II have been obtained under the assumption that the $\theta(1690)$ has $J^P = 2^{++}$. This experiment[11] finds equal likelihoods for 2^{++} and 0^{++} in contrast to earlier analyses by Crystal Ball and Mark III where spin 2 was favored over spin 0.[9,10]

3. $\iota(1460)$

The $\iota(1460)$ was discovered in the $K^0_S K^{\pm}\pi^{\mp}$ final state by Mark II[16] and has since been seen by several experiments studying J/ψ decays. As yet no other decay modes besides $K\bar{K}\pi$ final states have been observed. Nevertheless, the decay $J/\psi \to \gamma\iota \to \gamma K\bar{K}\pi$ is the largest radiative decay of the J/ψ (Table I) with the exception of the transition to the η_c which is about 2-3 times bigger. Figure 6 shows the $\iota(1460)$ in the DM2 experiment. The ι spin has been determined by the Crystal Ball group in an isobar analysis,[17] which assumes that the decay sequence is $\iota \to \delta\pi$, $\delta \to K\bar{K}$, and by Mark III performing a three–body helicity analysis which does not make this assumption.[18] Both analyses yield 0^{-+} for the iota.

Observation of the radiative decay of the $\iota(1460)$ into $\gamma\rho$ would be of great theoretical interest clarifying the nature of this state. Bag model calculations[19,20,21] which interpret the $\iota(1460)$ as a glueball with a $q\bar{q}$ admixture, predict $\Gamma_{\iota\to\gamma\rho^0}$ to lie in the range between 0.4 MeV and 1.6 MeV. A pole model of Palmer and Pinsky[22] predicts 3.5 MeV. If $\iota(1460)$ is a

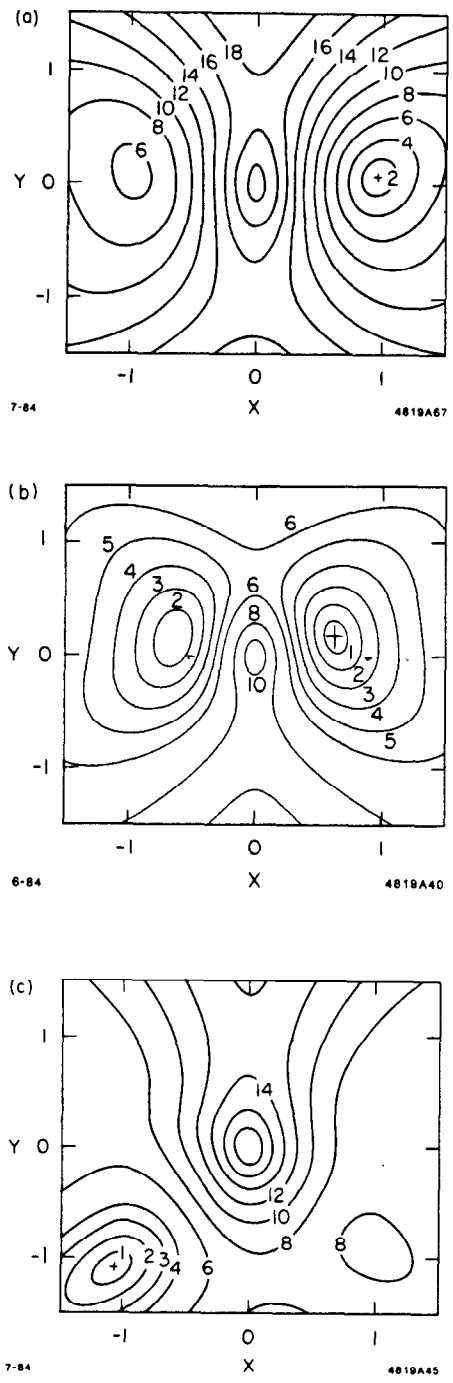

Fig. 5. Contour plots of polarisation fits to (a) f(1270), (b) $f'(1515)$, and (c) $\theta(1690)$ in an analysis of Mark III data.[9] $x = A_1/A_0$, $y = A_2/A_0$, where A_i are the production helicity amplitudes. The lines indicate areas of equal likelihood. The maximum of the likelihood function is marked by the cross.

radial $q\bar{q}$ excitation a smaller width is expected.[21,28] Three experiments have reported the observation of a resonance which decays into $\gamma\rho$ at a mass around 1.4 GeV. This state is about 1-2 σ lower in mass and has a width larger than that observed for $\iota \to K\bar{K}\pi$. Figure 7 shows the $\gamma\rho$ invariant mass distribution as measured by the Crystal Ball experiment. If this resonance is interpreted as $\iota(1460)$ and if $B(\iota \to K\bar{K}\pi) \approx 1$ then $\Gamma_{\iota\to\gamma\rho^0} = (1.9 \pm 0.7)$ MeV and, following most theoretical predictions, a significant $q\bar{q}$ component in the $\iota(1460)$ is likely.

TABLE II: Polarisation Parameters of f, f', and θ

		experimental					theoretical			
		PLUTO	Mark II	Crystal Ball	Mark III	DM2	Krammer	Körner	Li,Shen	Close
							Ref. 10	Ref. 11	Ref. 12	Ref. 13
f	$x = \frac{A_1}{A_0}$	0.6 ± 0.3	0.81 ± 0.16	0.88 ± 0.11	0.94 ± 0.10		0.76	0.77	0.66	0.87
	$y = \frac{A_2}{A_0}$	$0.3 \pm^{0.6}_{1.6}$	0.02 ± 0.15	0.04 ± 0.14	0.06 ± 0.11		0.54	0.55	0.04	0
	(ϕ_x, ϕ_y)		(0,0) fixed		$(\sim 0, \sim 0)$			$(2°, 4°)$		
f'	$x = \frac{A_1}{A_0}$				0.63 ± 0.10	1.08 ± 0.10	0.88	0.90		
	$y = \frac{A_2}{A_0}$				0.17 ± 0.20	0.19 ± 0.11	0.70	0.72		
	(ϕ_x, ϕ_y)				$(\sim 0, \sim 0)$			$(1.3°, 2.4°)$		
θ	$x = \frac{A_1}{A_0}$				-1.07 ± 0.20	-1.47 ± 0.21				
	$y = \frac{A_2}{A_0}$				-1.09 ± 0.25	-1.44 ± 0.20				
	(ϕ_x, ϕ_y)				$(\sim 0, \sim 0)$					

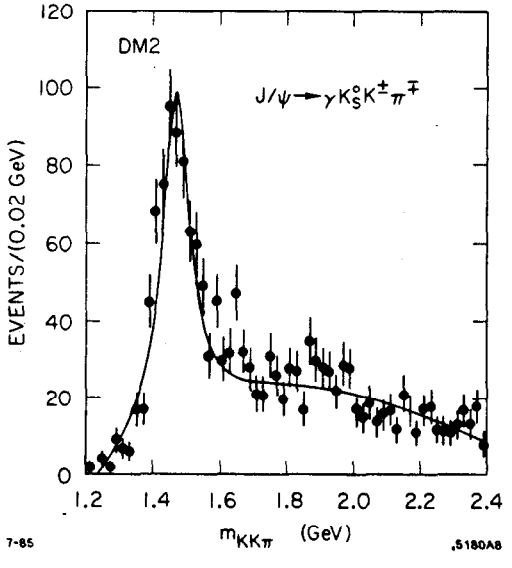

Fig. 6. $K\bar{K}\pi$ invariant mass distribution as observed by DM2.

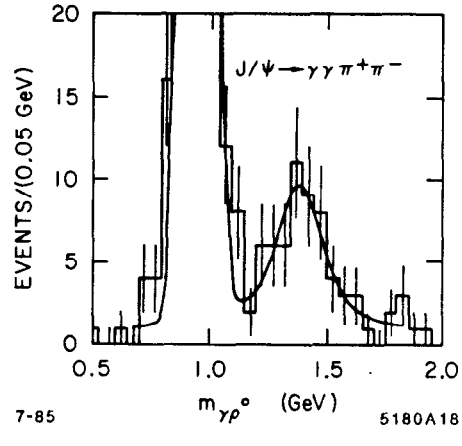

Fig. 7. Invariant $\gamma\rho$ mass distribution (Crystal Ball).

The question whether the $\iota(1460)$ decays to $\delta\pi$ is still a mystery. Although the Dalitz plot for the $K\bar{K}\pi$ decay mode and the $K\bar{K}$ invarant mass distribution are consistent with $\iota \to \delta\pi$, $\delta \to K\bar{K}$, no ι is found in the decay sequence $J/\psi \to \gamma\delta\pi$, $\delta \to \eta\pi$.

A strong argument in favour of a glueball interpretation for the $\iota(1460)$ is that, with the exception of one state, there is no room for additional states in the 0^{-+} $q\bar{q}$ groundstate

and radial excitation nonets. The 0^{-+} $q\bar{q}$ groundstate nonet is completed with $q\bar{q}$ states and the nonet of the first radial excitation is, except for its two center members, also reasonably well established. The $\eta(1275)$, a good candidate for one of the two states in the center of the radial excitation nonet, has been observed by Stanton et al.[24] , and has been confirmed recently by Ando et al. at KEK.[25] Orbital excitations are not possible for spin 0. Thus only one pseudoscalar state is missing to complete the 0^{-+} $q\bar{q}$ meson multiplets. A central question therefore is whether the $\iota(1460)$ could fill this hole and whether a radially excited $q\bar{q}$ state could be produced with a branching fraction as large as observed for the $\iota(1460)$. The discovery of even more pseudoscalar states in the same mass region (see section 4) necessarily implies that not all of them can fit into the $q\bar{q}$ picture and new physiscs must be employed for an explanation.

4. $J/\psi \rightarrow \gamma +$ Vector + Vector

Enhancements in $\rho\rho$ final states with masses below 2 GeV have been found in hadronic interactions[26] , in photon-photon collisions,[27] and in radiative J/ψ decays.[28] In $\phi\phi$ final states the g_T states near 2.2 GeV have been observed in $\pi^- p$ interactions.[7] Interpretations of these $\rho\rho$ and $\phi\phi$ enhancements include resonance production of $q\bar{q}$, $qq\bar{q}\bar{q}$, $q\bar{q}g$, and gg bound states.

The decay $J/\psi \rightarrow \gamma\rho^\circ\rho^\circ$ was first observed by Mark II.[28] The $\rho\rho$ mass distribution was found to be concentrated below 2 GeV with structure at 1.65 GeV. Several authors[29] have pointed out that if this structure was due to the $\theta(1690)$, the branching fraction for $J/\psi \rightarrow \gamma\theta(1690)$ would be $\approx 5 \times 10^{-3}$, a factor of three larger than that observed for $\eta\eta$ and $K\bar{K}$ final states, which would make a glueball interpretation of this state more likely.

Since the large $\rho\rho$ production cross section near threshold observed in $\gamma\gamma$ collisions and the $\rho\rho$ spectrum in radiative J/ψ decays bear some similarity, it has been proposed[30] that the underlying dynamics has the same origin. A spin-parity analysis[31] of $\gamma\gamma \rightarrow \rho^\circ\rho^\circ$ indicates that the $\rho\rho$ system is mostly 0^+ spin-parity below 1.7 GeV and mostly 2^+ above, but cannot rule out an isotropic model. Negative parity, however, is excluded by this analysis.

The Mark III group has analyzed $\gamma 4\pi$ final states using the two modes $\gamma\pi^+\pi^-\pi^+\pi^-$ and $\gamma\pi^+\pi^\circ\pi^-\pi^\circ$.[32] Both final states suffer a background contamination from $J/\psi \rightarrow 5\pi$ which can be subtracted on a statistical basis. The $m_{4\pi}$ invariant mass distributions after background subtraction are shown in Fig. 8 for both decay modes. Two peaks at masses of $\sim$ 1.55 GeV and $\sim$ 1.8 GeV are the striking features in these distributions. The statistical significance of these peaks can best be judged from the sum of the unsubtracted $m_{4\pi}$ distributions shown in Fig. 9. In a multichannel spin-parity analysis[32] a large $\rho\rho$ component is

found below 2 GeV, which appears to be predominantly pseudoscalar. The pseudoscalar $\rho\rho$ component is shown in Fig. 10 which is an average of $\rho^0\rho^0$ and $\rho^+\rho^-$. The two peak structure apparent in the 4π mass distributions (Fig. 9) is not visible in Fig. 10. The 0^- $\rho\rho$ component drops off at the location of the second peak at 1.8 GeV. The total branching fraction for the pseudoscalar $\rho\rho$ component below 2 GeV is

$$B(J/\psi \to \gamma X_{0^-}) \cdot B(X_{0^-} \to \rho\rho) = (4.7 \pm 0.3 \pm 0.9) \times 10^{-3}.$$

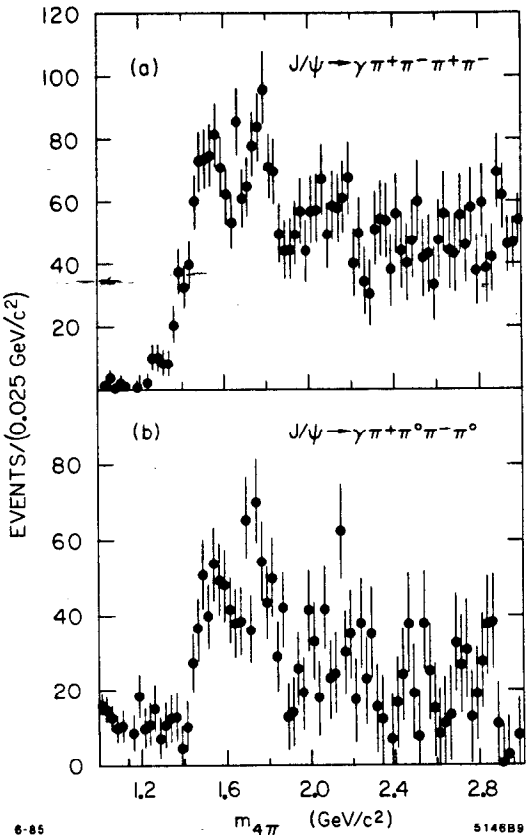

Fig. 8. Background subtracted invariant 4π mass distributions for (a) $J/\psi \to \gamma\pi^+\pi^-\pi^+\pi^-$ and (b) $J/\psi \to \gamma\pi^+\pi^0\pi^-\pi^0$ (Mark III).

No significant contribution from the 2^{++} channel is found at any mass resulting in the 90% confidence level upper limits

$$B(J/\psi \to \gamma\theta) \cdot B(\theta \to \rho\rho) \; < 5.5 \times 10^{-4}$$
$$B(J/\psi \to \gamma g_T) \cdot B(g_T \to \rho\rho) \; < 6.0 \times 10^{-4}.$$

Here g_T stands for the mass range 2.1 GeV $\leq$ $m_{\rho\rho}$ $\leq$ 2.4 GeV.

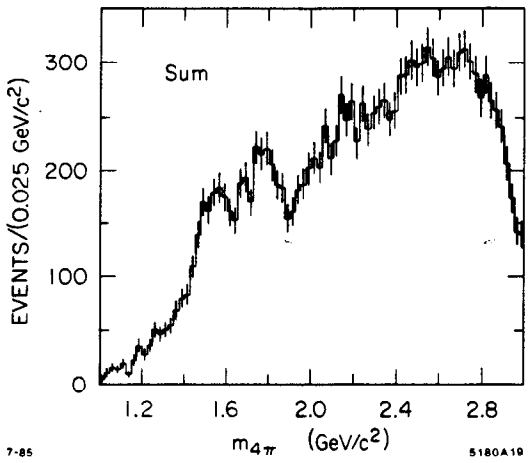

Fig. 9. Unsubtracted invariant 4π mass distribution. Shown is the sum of $J/\psi \to \gamma\pi^+\pi^-\pi^+\pi^-$ and $J/\psi \to \gamma\pi^+\pi^\circ\pi^-\pi^\circ$ (Mark III).

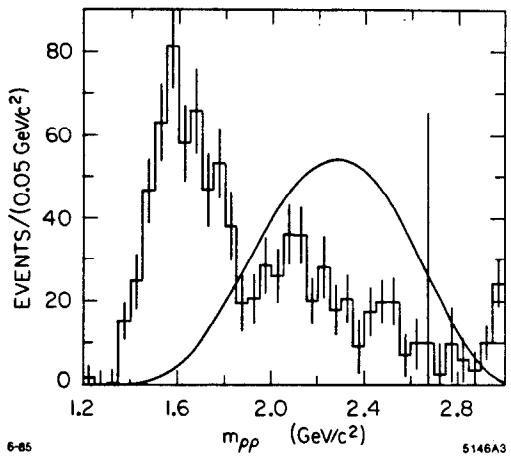

Fig. 10. The pseudoscalar $\rho\rho$ component, $m_{\rho\rho}$, extracted by a multichannel analysis from $J/\psi \to \gamma 4\pi$ (Mark III). The curve represents P-wave $\gamma\rho\rho$ phase space.

This analysis seems to add to the confusion already present in the pseudoscalar sector, introducing two new states of which at least the state lower in mass is presumably pseudoscalar. The obvious question, whether these are indeed two new states or whether they can be linked to already known resonances, will be addressed in section 6.

Mark III[33] and DM2 have searched for the decay $J/\psi \to \gamma\omega\omega$ in final states with four charged particles and five photons. The constraint imposed by the narrowness of the ω helps to extract an $\omega\omega$ signal from combinatorial and $\omega 4\pi$ backgrounds. The fact that the decays $J/\psi \to \pi^\circ\omega\omega$ and $J/\psi \to \omega\omega$ are forbidden by C-parity allows one to unambiguously identify the decay $J/\psi \to \gamma\omega\omega$. The $\omega\omega$ invariant mass distributions are shown in Figs. 11 and 12 for Mark III and DM2 data, respectively. The branching ratios obtained from the Mark III data are

$$B(J/\psi \to \gamma\omega\omega) = (1.76 \pm 0.09 \pm 0.45) \times 10^{-3} \quad \text{for} \quad m_{\omega\omega} < 3.1 \text{ GeV, and}$$
$$B(J/\psi \to \gamma\omega\omega) = (1.22 \pm 0.07 \pm 0.31) \times 10^{-3} \quad \text{for} \quad m_{\omega\omega} < 2.0 \text{ GeV.}$$

The spin-parity of the $\omega\omega$ system has been analysed by exploiting the information contained in the orientation of the ω decay planes[34] and by performing a multichannel spin-parity analysis similar to the one employed above for the $\rho\rho$ final state.[32,33] It is found that the $\omega\omega$ system below 2 GeV has predominantly 0^- spin-parity, very similar to the result for the $\rho\rho$ system. The upper limits for the 2^{++} states $\theta(1690)$ and g_T are

$$B(J/\psi \to \gamma\theta) \cdot B(\theta \to \omega\omega) < 2.4 \times 10^{-4}$$
$$B(J/\psi \to \gamma g_T) \cdot B(g_T \to \omega\omega) < 2.6 \times 10^{-4} \,,$$

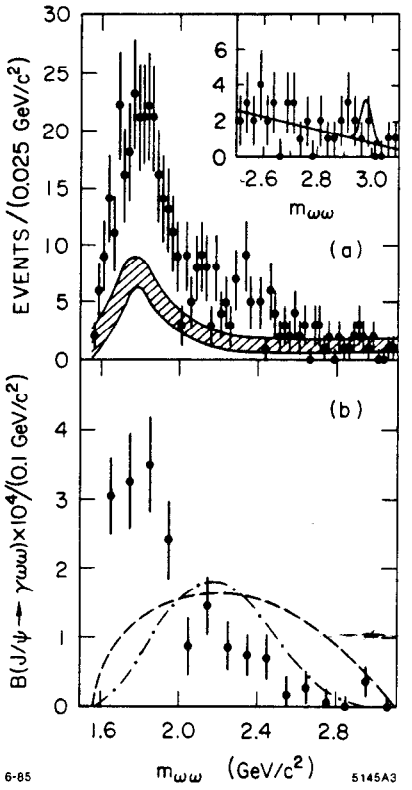

Fig. 11. (a) Invariant $\omega\omega$ mass distribution (Mark III). The band represents the background. The mass region from 2.5 GeV to 3.1 GeV is shown in the insert with the 90% C.L. curve for the η_c superimposed. (b) $B(J/\psi \to \gamma\omega\omega)$ as a function of $m_{\omega\omega}$. The curves represent S-wave (dashed) and P-wave (dashed-dotted) phase space.

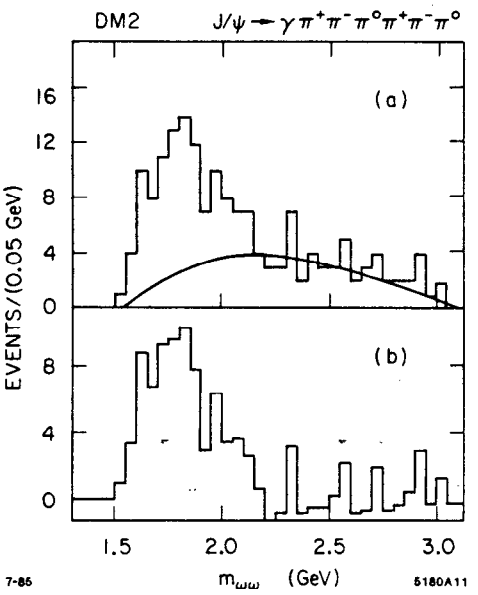

Fig. 12. (a) Invariant $\omega\omega$ mass distribution (DM2). The curve is the background estimate. (b) Background subtracted $\omega\omega$ mass distribution.

again using g_T for the mass range 2.1 GeV $\leq$ $m_{\omega\omega}$ $\leq$ 2.4 GeV.

Finally, the decay $J/\psi \to \gamma\phi\phi$ has been examined. This decay was used by the Mark III group to determine spin and parity of the η_c.[35] A severe decrease in detection efficiency towards lower $\phi\phi$ invariant masses due to kaon decays did not allow to place stringent limits on the g_T states, for which this final state is particularly interesting. The DM2 collaboration has substantially increased the kaon detection efficiency by loosening the TOF requirements. The preliminary $\phi\phi$ mass distribution thus obtained is shown in Fig. 13(a) together with the mass dependence of the detection efficiency (Fig. 13(b)). Figure 13(a) shows an indication of a peak at 2.2 GeV which, if it withstands further analysis, is very interesting for both the g_T states and for the $\xi(2200)$.

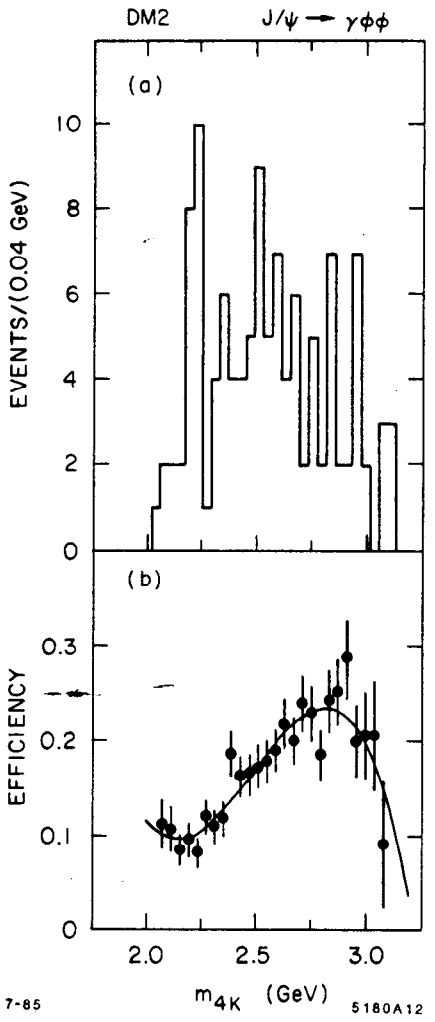

Fig. 13. (a) Invariant $\phi\phi$ mass distribution (DM2). (b) Detection efficiency for $J/\psi \to \gamma\phi\phi$ as a function of m_{4K}.

5. The Pseudoscalar Puzzle

Let me now introduce what I would like to call the "Pseudoscalar Puzzle in Radiative J/ψ Decays". As mentioned earlier, there is most likely only one more slot available to complete the 0^{-+} $q\bar{q}$ multiplets by finding the radially excited partner of η or η'. This state should be accessible in radiative decays of the J/ψ. Its production rate is expected to be less than or equal to the rate obtained for the groundstate members. Possible candidates for this state are abundantly available. Some of them are produced with large branching fractions. They are listed in the following.

- The largest radiative J/ψ decay ($B_\psi \cdot B_{KK\pi} \sim 5 \times 10^{-3}$) occurs to the $\iota(1460)$. Its spin is $J^{PC} = 0^{-+}$.[17,18]

- No $\iota(1460)$ is found in the $\eta\pi\pi$ final state, but instead a peak in the $\eta\pi\pi$ invariant mass distribution at 1.38 GeV, $\Gamma \sim 100$ MeV, is observed.[36] The spin of this state is still undetermined. The product branching fraction is $\sim 2 \times 10^{-3}$.
- In the decay of $J/\psi \to \gamma\gamma\rho$ the $\gamma\rho$ system shows a peak near 1.40 GeV with $\Gamma \sim$ 150 MeV. This state could be the $\iota(1460)$, although a systematically lower mass value has been observed in three different experiments. The spin-parity of the $\gamma\rho$ state is consistent with 0^-.[18] The branching fraction is 1×10^{-4}.
- Two peaks are found in $J/\psi \to \gamma\rho\rho$[32] . Their masses are ~ 1.55 GeV and ~ 1.8 GeV, both being about 70 to 100 MeV wide with branching fractions in the order of 2×10^{-3} for each peak. A pseudoscalar spin-parity assignment for at least the state at 1.55 GeV seems likely.
- In the decay $J/\psi \to \gamma\omega\omega$ a peak just above $\omega\omega$ threshold at 1.8 GeV is observed[33] whose spin-parity is predominantly pseudoscalar below 2 GeV. The branching ratio is $\sim 1 \times 10^{-3}$.

In the following section the possibility that some of these states have a common origin is explored.

6. A coupled channel analysis of $\iota(1460)$ decays

The Mark III group has performed a coupled channel analysis of $\iota(1460)$ decays to $K\bar{K}\pi$, $\rho\rho$, $\omega\omega$, and $\gamma\rho$. This analysis is primarily motivated by the need to understand the Breit–Wigner shapes of the peaks observed in $J/\psi \to \gamma\rho\rho$, but also by the hope to gain insight into the pseudoscalar puzzle. The main point is to note that the observed mass and width of a resonance may be different in different channels when threshold effects in some of the decay channels are important.

A combined description of the above listed channels is attempted by employing the ideas of the unitarized quark model[37] in a coupled channel analysis. In this model, the coupled channel Breit–Wigner amplitude, i.e. the propagator function for an unstable particle, is written as

$$BW_{cc}(s) \propto \left[m_o^2 + Re\Pi(s) - s + iIm\Pi(s)\right]^{-1}, \tag{1}$$

where m_o is defined as the 'bare' mass and $\Pi(s)$ describes the loop corrections to the stable particle propagator.[37] The unitarity condition defines

$$-Im\Pi(s) = m_o \sum_a \Gamma_a(s) = m_o \sum_a g_a p_a F_a^2(q_a), \tag{2}$$

where for each channel a with two body cm–momentum q_a, Γ_a is the decay width, g_a a

coupling coefficient, and $F_a(q_a)$ a phenomenological form factor which introduces damping at high q_a values. The p_a represent the phase space factors for each channel. The Γ_a for the individual channels are described in the following.

$K\bar{K}\pi$: The observed $K\bar{K}$ invariant mass distribution is well parametrized by a Breit–Wigner distribution $B_\delta(m)$ times 3-body phase space, properly normalized,

$$\Gamma_{K\bar{K}\pi}(s) = g_{K\bar{K}\pi} \int dm' \mid B_\delta(m') \mid^2 \cdot \frac{dR_3}{dm'} \cdot \frac{q_{K\bar{K}}(m')}{\sqrt{s}} \cdot F^2(q_{K\bar{K}}(m')), \tag{3}$$

where $q_{K\bar{K}}$ is the momentum of the $K\bar{K}$ system in the $K\bar{K}\pi$ rest frame. For $B_\delta(m)$ Flatté's parametrization[38] is used. This parametrization adequatly describes the $K\bar{K}$ mass distribution of the $\iota \to K\bar{K}\pi$ decay.[18] It should be emphasized that, although the $K\bar{K}\pi$ channel is parametrized using the δ, this does not imply that the decay $\iota \to K\bar{K}\pi$ actually proceeds through $\iota \to \delta\pi$, $\delta \to K\bar{K}$.

An exponential form factor is used for $F(q)$,[37] $F(q) = exp(-q^2/q_1^2)$, with $q_1 = 0.7$ GeV/c.

$$\begin{aligned} \rho\rho: \quad \Gamma_{\rho\rho}(s) = & g_{\rho\rho} \int ds_{12} \frac{q_\pi^3(s_{12})}{\sqrt{s_{12}}} \frac{d\Omega_{12}}{4\pi} \int ds_{34} \frac{q_\pi^3(s_{34})}{\sqrt{s_{34}}} \frac{d\Omega_{34}}{4\pi} \\ & \times \frac{Q^3_{\pi_1\pi_2}}{\sqrt{s}} \cdot \sin^2\theta_1 \sin^2\theta_3 \sin^2\chi \cdot \left(\frac{3}{2}\right)^2 \cdot 2 \\ & \times \frac{1}{2} \mid \widetilde{B}_\rho(s_{12}) \widetilde{B}_\rho(s_{34}) F(Q_{\pi_1\pi_2}) - \widetilde{B}_\rho(s_{14}) \widetilde{B}_\rho(s_{23}) F(Q_{\pi_1\pi_4}) \mid^2 , \end{aligned} \tag{6}$$

where s_{ij}, $i,j = 1-4$, are the center-of-mass energies squared for the $\pi\pi$ systems; q_π and $\theta_{1,3}$ are the π – cm momentum and polar angle in the respective $\pi\pi$ rest frames; $Q_{\pi_i\pi_j}$ is the momentum of $\pi\pi$–system i,j in the 4π–cms; χ is the angle between the ρ decay planes; $\widetilde{B}_\rho = B_\rho/q_\pi(s)$ where B_ρ is the ρ – Breit–Wigner amplitude.[39] Note that the matrix element is invariant under the interchange of pions 1 and 3 and that the decay of a 0^- resonance to $\rho\rho$ leads to destructive interference in the sum of the Breit-Wigner amplitudes.[32] For $\omega\omega$:

$$\Gamma_{\omega\omega}(s) = g_{\omega\omega} \cdot \frac{q_\omega^3}{\sqrt{s}} \cdot F^2(q_\omega), \tag{7}$$

and for $\gamma\rho$:

$$\Gamma_{\gamma\rho^0}(s) = g_{\gamma\rho} \cdot \frac{q_\rho^3}{\sqrt{s}} \cdot F^2(q_\rho). \tag{8}$$

The analyticity of $\Pi(s)$ connects $Re\,\Pi(s)$ and $Im\,\Pi(s)$ by the dispersion relation

$$Re\,\Pi(s) = \frac{1}{\pi} \int_{s_0}^{\infty} \frac{Im\,\Pi(s')}{s'-s}\, ds' \quad , \tag{9}$$

where the lower bound s_0 is given by the $K\bar{K}\pi$ threshold.

The coupled channel Breit–Wigner of Eq. (1) has 5 parameters: m_o, $g_{KK\pi}$, $g_{\rho\rho}$, $g_{\omega\omega}$, and $g_{\gamma\rho}$. Mark III has used m_o, $\Gamma_{KK\pi}$, the partial width in the $K\bar{K}\pi$ channel and the coupling ratios $r_1 = g_{\rho\rho}/g_{KK\pi}$, $r_2 = g_{\rho\rho}/g_{\omega\omega}$, and $r_3 = g_{\rho\rho}/g_{\gamma\rho}$. The Vector Dominance Model (VDM) predicts for the ratio of $\rho\rho$ to $\gamma\rho$ couplings the value $e^2/f_\rho^2 \cdot \frac{3}{2} \approx 400$, where the factor $\frac{3}{2}$ takes into account the $\rho\rho$ isospin and the fact that either ρ° can become a photon. The ratio of $\rho\rho$ to $\omega\omega$ couplings is expected to be 3 from SU(3) symmetry.

Figure 14 indicates the distortions of the Breit–Wigner shapes due to phase space and coupled channel effects considering $K\bar{K}\pi$, $\rho\rho$, $\omega\omega$, and $\gamma\rho$ with parameters $m_o = 1.48$ GeV, $\Gamma_{KK\pi} = 0.100$ GeV, $r_1 = 35$, $r_2 = 3$, $r_3 = 400$. Figure 14(a) displays the Breit–Wigner shapes and (b) $\Gamma_a(s)$ for these channels as well as $m_o^2 + Re\,\Pi(s)$ as obtained by eqn. (9). Mass shifts and changes in shape are different for the individual channels due to phase space and coupled channel effects. The $\rho\rho$ Breit–Wigner is pushed to higher masses and appears to have a larger tail as compared to $K\bar{K}\pi$. The Breit–Wigner shape for the $\omega\omega$ channel is strongly distorted. $Re\,\Pi(s)$ shows a smooth dip at about 1.5 GeV, where the $\rho\rho$ and $\omega\omega$ channels open up.

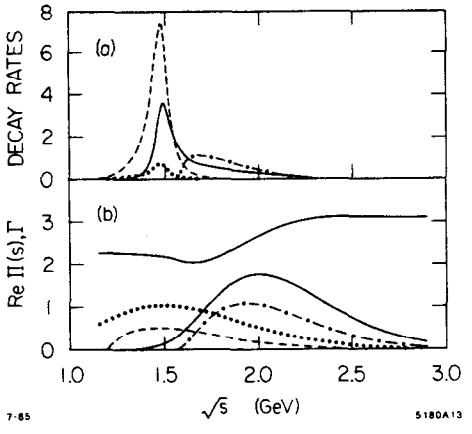

Fig. 14. (a) Coupled channel Breit–Wigner amplitude squared for the channels $K\bar{K}\pi$ (dashed), $\rho\rho$ (solid), $\omega\omega$ (dashed–dotted), and $\gamma\rho$ (dotted) in arbitrary units. The parameters are described in the text. (b) Re $\Pi(s)$ and Γ_a as a function of $\sqrt{s}$. The curve for $\Gamma_{\gamma\rho}$ (dotted line) is multiplied by 100.

The coupled channel ansatz described in eqs. (1) – (9) is fit to the MARK III data for the four final states shown in Fig. 15. Figure 15(a) is the sum of $J/\psi \to \gamma K^+K^-\pi^\circ$ and $J/\psi \to \gamma K_s^\circ K^\pm\pi^\mp$. Figure 15(b) shows the data for $J/\psi \to \gamma\pi^+\pi^-\pi^+\pi^-$, where the background from $\psi \to \pi^\circ 4\pi$ has been subtracted.[82] The $0^-\rho\rho$ contribution to $J/\psi \to \gamma 4\pi$ amounts to $\sim$ 50% below 2 GeV.[82] Figure 15(c), (d) show background-subtracted mass distributions for the decays $J/\psi \to \gamma\gamma\rho$ and $J/\psi \to \gamma\omega\omega$. The distributions are normalized according to their relative efficiencies $\epsilon_{K\bar{K}\pi} : \epsilon_{\rho\rho} : \epsilon_{\omega\omega} : \epsilon_{\gamma\rho} = 0.4 : 1 : 1.15 : 4.0$. The systematic uncertainty in this normalization is 40%.

The fit is performed assuming 2 coupled channel Breit–Wigner amplitudes centered at $\sim$ 1.5 GeV and $\sim$ 1.8 GeV allowing for interference and assuming that the 1.8 GeV peak is

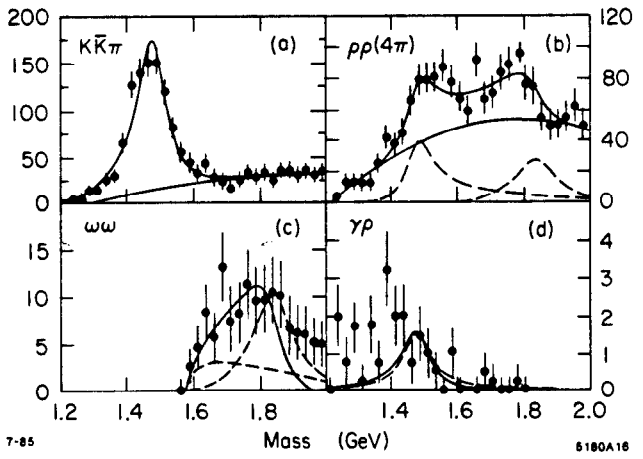

Fig. 15. Invariant mass distributions for (a) $K\bar{K}\pi$, (b) $\rho\rho$, (c) $\omega\omega$, and (d) $\gamma\rho$ (Mark III) corrected for relative efficiencies (arb. units, 0.025 GeV bins). The curves represent the results of the coupled channel analysis as described in the text.

also pseudoscalar. A factor E_γ^3, where E_γ is the energy of the radiative photon, is included for pseudoscalar X in $J/\psi \to \gamma X$. The lower mass Breit–Wigner is assumed to couple to all four channels. The second Breit–Wigner is assumed to couple only to $\rho\rho$, $\omega\omega$, and $\gamma\rho$. Background terms are included only for $K\bar{K}\pi$ and $\rho\rho$. A possible contribution from the η' decaying to $\gamma\rho$, $\rho\rho$, and $\omega\omega$, which introduces an additional parameter $g_{\eta'\rho\rho}/g_{\iota\rho\rho}$ is also included.[40] Except for the relative coupling strengths $g_{\rho\rho}/g_{\omega\omega}$ and $g_{\rho\rho}/g_{\gamma\rho}$, there is no additional parameter fitting shape and magnitude of the $\omega\omega$ and $\gamma\rho$ mass distributions.

The fit results are shown by the superimposed curves in Fig. 15. They demonstrate that the lower part of the $\rho\rho$ mass distribution can be explained by a resonance below $\rho\rho$ threshold. A strong candidate for this resonance is the $\iota(1460)$. The constraints of the coupled channel analysis leave the ι parameters, as determined from the $K\bar{K}\pi$ channel,[18] unaffected. The $\omega\omega$ invariant mass distribution can also be described by this ansatz. The shape of the $\gamma\rho$ invariant mass distribution is not well reproduced. Since phase space effects are much less important in this channel than for the $\rho\rho$ and $\omega\omega$ channels the Breit–Wigner peak value must be the same as for the $K\bar{K}\pi$ decay and cannot be shifted to lower masses. The $\chi^2/d.o.f$ of the fit is 1.42 for all four histograms and 1.2 for Fig. 15(b).

The analysis is sensitive to the choice of the form factor $F(q)$ in that it modifies the definition of the coupling coefficients g_a. The qualitative features of the fit, however, remain unchanged under a change of form factors. In the absence of a dynamical model the ratios of coupling coefficients can be interpreted only for channels with the same coupling types like for the Vector – Vector channels, i.e. $g_{\rho\rho}/g_{\omega\omega}$ and $g_{\rho\rho}/g_{\gamma\rho}$, but not $g_{\rho\rho}/g_{KK\pi}$. Because the

momenta for the three Vector – Vector channels are different at fixed $\sqrt{s}$, different suppression factors in each channel are introduced by the form factor which affect the ratio of coupling coefficients chosen by the fit. After correcting for this effect one finds $g_{\rho\rho}/g_{\omega\omega} = 5.0 \pm 0.7$ which should be compared to the value of 3 expected from SU(3) symmetry. For $g_{\rho\rho}/g_{\gamma\rho}$ a value of 3300 ± 600 is the result of the fit. While the $g_{\rho\rho}/g_{\omega\omega}$ ratio is less sensitive to the exact choice of $F(q)$, because m_ρ and m_ω are almost equal, a softer form factor would greatly reduce the value of $g_{\rho\rho}/g_{\gamma\rho}$ to smaller values. The VDM predicted value of 400, however, although not excluded, seems to be too small to describe the observed $\gamma\rho$ decay rate.

The fit attributes (300 ± 30) $\rho\rho$ events and (45 ± 15) $\omega\omega$ events to the $\iota(1460)$. This leads to the following preliminary branching fractions

$$B(J/\psi \to \gamma\iota) \cdot B(\iota \to \rho\rho) \approx (1.5 \pm 0.2) \times 10^{-3}.$$
$$B(J/\psi \to \gamma\iota) \cdot B(\iota \to \omega\omega) \approx (0.3 \pm 0.1) \times 10^{-3}.$$

For the $X(1800)$ peak one finds

$$B(J/\psi \to \gamma X(1800)) \cdot B(X(1800) \to \rho\rho) \approx (1.0 \pm 0.2) \times 10^{-3}.$$

The total production branching fraction of the ι, including the decays to $\rho\rho$ and $\omega\omega$, then increases by about 40% to

$$B(J/\psi \to \gamma\iota(1460)) \; > \; (6.9 \pm 0.4 \pm 1.0) \times 10^{-3},$$

where the Mark III value has been used for $\iota \to K\bar{K}\pi$.

The $\eta\pi\pi$ invariant mass distribution after a δ – cut, requiring the $\eta\pi$ invariant mass within 30 MeV about the $\delta(980)$ mass, is shown in Fig. 16. This distribution is used as an additional channel to test the following two hypotheses: (a) The mass peak seen in $\eta\pi\pi$ is not the $\iota(1460)$ and is therefore different from the peak seen in the $K\bar{K}\pi$ spectrum but has the same origin as the peaks seen in $\gamma\rho$, $\rho\rho$, and $\omega\omega$; (b) the $\eta\pi\pi$ signal is the $\iota(1460)$. Testing for hypothesis (a) checks also whether the ι is the preferred candidate for the lower part of the $\rho\rho$ spectrum or whether another resonance below $\rho\rho$ threshold could fulfill this role. To test for (a) the $\eta\pi\pi$ distribution is substituted for the $K\bar{K}\pi$ distribution in Fig. 15(a) and the decay sequence $X(1380) \to \delta\pi$, $\delta \to \eta\pi$ is assumed. A fit with this hypothesis yields a significantly worse χ^2 in the $\rho\rho$ distribution. The conclusion is that the $\iota(1460)$ is the preferred candidate for the state below $\rho\rho$ threshold that is responsible for the peak at 1.55 GeV in Fig. 15(b). Hypothesis (b) is tested by adding the $\eta\pi\pi$ mass distribution to the four channels of Fig. 15 and requiring that the mass bump at 1.380 MeV in $\eta\pi\pi$ corresponds to the $\iota(1460)$. The

result with an assumed 10% $\eta\pi\pi/K\bar{K}\pi$ coupling ratio is superimposed in Fig. 16. The peak at 1.380 GeV cannot be described by the curve. One concludes that the mass bump X(1380) in the decay $J/\psi \to \eta\pi\pi$ is not the $\iota(1460)$.

Achasov and Shestakov[40] have analyzed an earlier version of the Mark III data[41] and have come to similar conclusions.

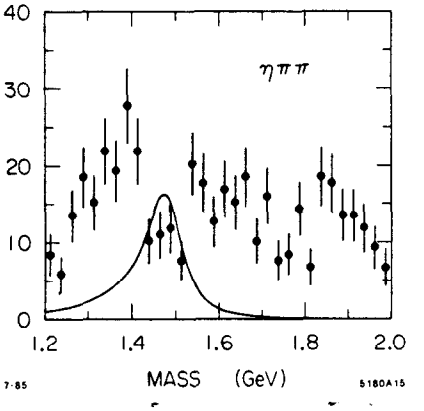

Fig. 16. Invariant $\eta\pi\pi$ mass distribution (Mark III) corrected for relative efficiency (arb. units, 0.025 GeV bins). The curve represents the iota when the decay $\iota \to \delta\pi$, $\delta \to \eta\pi$ is included in the coupled channel analysis assuming a 10% $\eta\pi\pi/K\bar{K}\pi$ coupling.

7. Summary and Conclusions

Preliminary results of a coupled channel analysis of $\iota(1460)$ decays have been presented in the previous section. According to this analysis the glueball interpretation of the $\iota(1460)$ becomes more likely. The lower part of the $\rho\rho$ invariant mass distribution is attributed to a resonance below nominal $\rho\rho$ threshold. The preferred candidate for this resonance is the iota. The analysis also shows that the iota decays to $\omega\omega$. With these new ι decay modes the branching fraction $B(J/\psi \to \gamma\iota)$ increases to a value of about 0.7%, which is roughly half of the branching fraction for $J/\psi \to \gamma\eta_c$ and is by far the largest radiative decay of the J/ψ to non-$c\bar{c}$ states. The other glueball candidate, $\theta(1690)$ is produced with $B_\psi \cdot B_{K\bar{K},\pi\pi,\eta\eta} \approx 1.6 \times 10^{-3}$. The polarisation of the θ is dramatically different from that of the $q\bar{q}$ tensor mesons f(1270) and $f'(1515)$. Both $\theta(1690)$ and $\iota(1460)$ are observed in several decay modes according to the coupled channel analysis. The final states contain strange and non-strange quarks. The spins 2^{++} and 0^{-+} agree with the spin expectation for the gg system in $J/\psi \to \gamma gg$ obtained from a perturbative QCD calculation.[5] The corresponding 2^{++} and 0^{-+} $q\bar{q}$ groundstate multiplets are well established. For 0^{-+} also the first radial excitation is nearly complete leaving room for only one more pseudoscalar. Assigning the $\iota(1460)$ to this missing state would imply that the radially excited partner of η or η' is produced with an almost an order of magnitude larger branching fraction than the η. Searches for $\theta(1690)$ and $\iota(1460)$ in hadronic decays of the J/ψ are reported by J. E. Augustin at this conference.[42] Both θ and $\iota(1460)$ seem to become stronger glueball candidates as time goes on.

The quest of the $\xi(2200)$ state will regain attention when the new data sample of about 3×10^6 J/ψ is analysed by Mark III.

Acknowledgements

My special thanks go to Toby Burnett for a long period of joint analysis efforts. I would like to thank R. Partridge, T. Schalk, and especially G. Wolf for their help preparing this talk and for fruitful discussions. I also wish to acknowledge helpful conversations with R. Blankenbecler. I am grateful to J. E. Augustin and L. Montanet for their open position on the arrangement of the talks.

References

1. A recent review has been given by S. Sharpe, Proc. of Vanderbuilt Conference on High Energy e^+e^- Interactions, Vanderbuilt 1984; M. Chanowitz, Nucl. Phys. *B*222, 211 (1983) and references therein; C. E. Carlson and T. H. Hansson, Phys. Rev. *D*27, 1556 (1983), and Phys. Rev. *D*30, 1594 (1984); K. Ishikawa, A. Sato, G. Schierholz, and M. Teper, Nucl. Phys. *C*21, 167 (1983) and references therein; J. M. Cornwall and A. Soni, Phys. Lett. 120*B*, 431 (1983).
2. R. M. Baltrusaitis *et al.*, SLAC–PUB–3435, submitted to Phys. Rev. D. (1985).
3. D. Robson, Nucl. Phys. *B*130, 328 (1977).
4. V. A. Novikov, M. A. Shifman, A. I. Vainshtein, and V. I. Zakharov, Nucl. Phys. *B*191, 301 (1981); A. Soni, Phys. Rev. *D*29, 1424 (1984); M. S. Chanowitz, Proceedings on the XIV International Symposium on Multiparticle Dynamics at High Energies, Lake Tahoe (1983).
5. A. Billoire, R. Lacaze, A. Morel, and H. Navelet, Phys. Lett. 80*B*, 381 (1979).
6. E. D. Bloom, Aspen Winter Physics Conference, Jan. 1985 and SLAC-PUB-3573, (1985).
7. A. Etkin *et al.*, Phys. Rev. Lett. 49, 1620 (1982).
8. K. F. Einsweiler, Int. Europhys. Conf. on High Energy Physics, Brighton, July (1983); D. Hitlin, Int. Symp. on Lepton and Photon Interactions, Cornell, August (1983).
9. K. F. Einsweiler, Ph.D. Thesis, SLAC–272, (1984).
10. C. Edwards *et al.*, Phys. Rev. Lett. 48, 458 (1982).
11. J. E. Augustin, private communication.
12. M. Krammer, Phys. Lett. 74*B*, 361 (1978).

13. J. G. Körner, J. H. Kühn, and H. Schneider, Phys. Lett. 120*B*, 444 (1983);
J. G. Körner, M. Krammer, J. H. Kühn, and H. Schneider, Nucl. Phys. *B*229, 115 (1983).

14. B. A. Li and Q. X. Shen, Phys. Lett. 126*B*, 125 (1983).

15. F. E. Close, Phys. Rev. *D*27, 311 (1983).

16. D. L. Scharre *et al.*, Phys. Lett. 97*B*, 329 (1980).

17. C. Edwards *et al.*, Phys. Rev. Lett. 49, 259 (1982).

18. J. D. Richman, Ph.D. Thesis, CALT-68-1231, (1985).

19. S. Iwao, Nuov. Cim. Lett. 35, 209 (1982); C. E. Carlson and T. H. Hansson, Nucl. Phys. *B*199, 441 (1982).

20. T. Barnes and F. E. Close, Rutherford Preprint, RAL-84-055, (1984).

21. J. F. Donoghue, Phys. Rev. *D*30, 114 (1984).

22. W. F. Palmer and S. S. Pinsky, Phys. Rev. *D*27, 2219 (1982);
W. F. Palmer, S. S. Pinsky, and C. Bender, Phys. Rev. *D*30, 1002 (1984).

23. S. Godfrey and N. Isgur, Toronto Preprint, Print-840036-Rev, (1984), and remarks in Ref. 18.

24. N. R. Stanton *et al.*, Phys. Rev. Lett. 42, 346 (1979).

25. A. Ando *et al.*, KEK Preprint 85-15, (1985).

26. A. Bettini *et al.*, Nuovo Cim. 42, 695 (1966);
H. Braun *et al.*, Nucl. Phys. *B*30, 213 (1971).

27. R. Brandelik *et al.*, Phys. Lett. 97*B*, 448 (1980); D. L. Burke *et al.*, Phys. Lett. 103*B*, 153 (1981); H. J. Behrend *et al.*, Z. Phys. *C*21, 205 (1984).

28. D. L. Burke *et al.*, Phys. Rev. Lett. 49, 632 (1982).

29. M. S. Chanowitz, Invited Talk at the XIV'th International Conference on Multiparticle Dynamics at High Energies, Lake Tahoe, (1983);
J. F. Donoghue, Invited Talk at the XXI'th International Conference on High Energy Physics, Paris, (1982).

30. B. A. Li and K. F. Liu, Phys. Rev. *D*30, 613 (1984), and Phys. Lett. 134*B*, 128 (1984).

31. M. Althoff *et al.*, Z. Phys. *C*16, 13 (1982).

32. R. M. Baltrusaitis *et al.*, SLAC–PUB–3682, submitted to Phys. Rev. D. (1985).

33. R. M. Baltrusaitis *et al.*, SLAC–PUB–3681, submitted to Phys. Rev. Lett. (1985).

34. N. P. Chang and C. T. Nelson, Phys. Rev. Lett. 40, 1617 (1978);
T. L. Trueman, Phys. Rev. *D*18, 3423 (1978).

35. R. M. Baltrusaitis *et al.*, Phys. Rev. Lett. 52, 2126 (1984).

36. W. Toki, 11th SLAC Summer Inst. on Particle Physics,(1983) and SLAC-PUB-3262;
J. J. Becker, Ph.D. Thesis, U. of Illinois, (1984). SLAC-PUB-3262;

37. N. A. Tornqvist, Ann. Phys. 123, 1 (1979); M. Roos and N. A. Tornqvist, Z. Phys. *C*5, 205 (1980).

38. S. Flatté, Phys. Lett. 63*B*, 228 (1976).

39. J. D. Jackson, Nuovo Cim. 34, 1644 (1964).

40. N. N. Achasov, G. N. Shestakov, Phys. Lett. 156*B*, 434 (1985).

41. N. Wermes, Invited Talk presented at the XIXth Recontre de Moriond, La Plagne, (1984), and SLAC–PUB–3312, (1984).

42. J. E. Augustin, Invited Talk presented at this conference, (1985).